DOI: 10.1021/ma100327p

Macromolecules
ARTICLE

Stimuli Responsive Peptide Conjugated Polymer Nanoparticles

Rutger J. I. Knoop,[†] Matthijs de Geus,[†] Gijs J. M. Habraken,[†] Cor E. Koning,[†] Henning Menzel,[‡] and Andreas Heise*,[†,§]

[†]*Technische Universiteit Eindhoven; Den Dolech 2, P.O. Box 513, 5600 MB Eindhoven, The Netherlands,* [‡]*Technische Universität Braunschweig, Institut für Technische Chemie, Hans-Sommer-Str. 10, 38106 Braunschweig, Germany, and* [§]*Dublin City University, School of Chemical Sciences, Dublin 9, Ireland*

Received February 9, 2010; Revised Manuscript Received March 31, 2010

ABSTRACT: We have investigated a novel approach to well-defined peptide-decorated cross-linked nanoparticles. The particles were obtained from well-defined poly(γ-benzyl-L-glutamate-*b*-styrene) block copolymers with active nitroxide end-groups by reaction with divinylbenzene (DVB). The block length ratio and the amount of cross-linker (DVB) were systematically varied. Molecular weights of the cross-linked particles up to 548 000 g/mol with polydispersities around 1.5 were confirmed by size-exclusion chromatography. A clear dependence of the molecular weight from the block length ratio and the amount of cross-linker was observed. This was confirmed by dynamic light scattering results revealing the formation of nanoparticles up to 21 nm in size. The core−shell structure was evident from the TEM micrographs. Further deprotection of the peptide shell yielded water-soluble pH-responsive nanoparticles with a poly(L-glutamic acid) shell and a polystyrene core. Cryo-TEM micrographs confirmed the presence of individual core−shell particles in the aqueous solution.

Introduction

The covalent conjugation of peptides and synthetic polymers provides the opportunity to design novel materials with the combined properties of both systems.[1] The peptide segment, for example, can provide biological functionality or hierarchical organization by self-assembly, whereas the synthetic polymers can add a wide range of properties by the choice of monomers. The ability to realize material properties not achievable by either of the systems alone already led to interesting applications of biohybrid polymers in drug delivery,[2−4] as mechanical property enhancers,[5,6] and in biomineralization.[7,8] Most examples of peptide−synthetic polymer conjugates are block copolymers in which the peptide segment is a natural protein or a synthetic polypeptide. Advances in the synthesis and application of these hybrid materials were recently reviewed by Klok.[9]

An emerging class of hybrid materials is bioconjugated nanoparticles, which have created increased interest in various medical application areas often referred to as nanomedicine. Materials combining inorganic nanoparticles with protein building blocks are for example investigated for sensor and biomedical diagnostic applications. Gold and silica nanoparticles conjugated with polypeptides or antibodies have been employed in a variety of investigations aiming at point-of-care devices.[10−13] Another direction of research on protein nanoparticles is the development of smart responsive materials. Liedberg showed that selected polypeptides immobilized on gold nanoparticles respond to the concentration of zinc ions in the solution by a change in peptide folding, causing the particles to reversibly aggregate.[14]

Our interest is in the development of bioconjugated nanoparticles entirely based on soft materials in which the particle-forming core is a cross-linked polymer forming the bases of core cross-linked core−shell nanoparticles. The advantage of a polymeric core is the flexibility in the design of the core properties by the choice of the monomeric building blocks. Functionalities and guest molecules like drugs or markers can thus be introduced into the core for various applications, for example, for drug delivery or biomedical diagnostics similar to inorganic nanoparticles. The aim of the work reported in this paper was the development of a generic synthetic approach for the formation of stable functional polymeric polypeptide responsive nanoparticles. Synthetic polypeptides are ideal materials to mimic natural peptides in these applications. They are readily accessible by ring-opening polymerization of amino acid *N*-carboxy anhydrides (NCA) and have been employed in the synthesis of bioconjugated block copolymers, which display interesting self-assembly behavior owing to the noncovalent interaction of the polypeptide blocks.[15−23] Synthetic core−shell polypeptide assemblies have already been applied in responsive and biomedical materials. Suslick, for example, reported the formation of noncovalent poly(glutamic acid) (PGA) core−shell microspheres targeting drug delivery applications.[24] Moreover, drug-loaded micelles from poly(ethylene glycol) conjugated poly(L-glutamic acid) (PGA) entered clinical drug delivery trials.[25] However, a general limitation of micelles is their dynamic nature, which leads to instabilities at high temperature, low concentrations, and under certain changes in solvent conditions. Stabilization of the polymeric micelles by cross-linking either its core or shell can overcome this limitation and has been applied to conventional micelles from amphiphilic block copolymers.[26] Cross-linked micelles are stable below the critical micelle concentration of the block copolymer, can be isolated and redissolved as stable nanoparticles, and are less likely to collapse, for example in the bloodstream. As a result, cross-linking can lead to increased circulation times, allowing drugs to be administered over longer period of time.[27] Irrespective of the location of the cross-links, these methods rely on the ability to initially form a micelle, which depends on the amphiphilic balance of the block copolymer. In a different approach, amphiphilic polystyrene/PGA block copolymers were recently employed by Rodriguez-Hernandez in a precipitation polymerization of styrene/divinylbenzene in aqueous medium.[28] The

*To whom correspondence should be addressed.

 Published on Web 04/14/2010

obtained core−shell particles had a size of 3−4 μm and responded to pH changes. However, the peptide-containing block copolymers were not covalently bound but only incorporated in the polystyrene microspheres.

We therefore adopted a different approach, which is based on reports that cross-linked (star) polymers can be formed by the addition of divinyl monomers, e.g., divinylbenzene, during a controlled radical polymerization.[29−31] In this paper we demonstrate that this approach can be applied for the synthesis of bioconjugated core cross-linked nanoparticles. We systematically investigated the synthetic conditions for the formation of the nanoparticles and the availability of the polypeptide nanoparticle to respond to an external stimulus, i.e., change in solvent pH.

Experimental Section

Materials. Methanol (abs. a.r.), diethyl ether (97%), chloroform (99+%) stabilized with ethanol for analysis, toluene (a.r), dry THF from solvent system, dichloromethane (a.r. stabilized with amylene) *N,N*-dimethylformamide (99%, extra dry), ethanol (abs.), ethyl acetate (a.r.), and *n*-heptane (a.r.) were obtained from Biosolve and were used as received unless stated otherwise. DMSO was obtained from Aldrich. Ethyl acetate was purified by distillation from CaH_2. Zinc dust (< 10 μm, 98%, Aldrich), $MgSO_4$ (pure, Aldrich), NH_4OH (32%, Aldrich), $Cu(OAc)_2$ (Aldrich), vinylbenzyl chloride (> 90%, Aldrich), $NaBH_4$ (99%, Aldrich), 4-*tert*-butylcatechol (Aldrich), lithium aluminum hydride (1.0 M in THF, Aldrich), 2-methyl-2-nitropropane (99%, Aldrich), isopropylmagnesium chloride (2.0 M in THF, Aldrich), α-pinene (98%, Aldrich), R,R-Jacobsen catalyst (98%, Acros), sodium azide (99%, Acros), di-*tert*-butyl peroxide (99%, Acros), ammonium chloride (+99%, Fluka), dibenzo-18-crown-6 (Fluka), benzaldehyde (+99%, VWR), HCl (32%, VWR), and γ-benzyl-L-glutamate ester (Sigma) were used as received. Styrene (99%, Aldrich) and anisole (99.7% anhydrous, Aldrich) were distilled before use. The bifunctional nitroxide initiator was synthesized following a literature procedure.[32]

Methods. SEC analysis with DMF (60 °C, 0.1 M LiBr) was carried out using a Waters 2695 Alliance pump + injector, equipped with a Waters 996 photodiode array UV detector, Viscotec RALS (right angle light scattering) detector, Viscotek 250 dual detector viscosity detection and differential refractive index detection, and a Waters 2414 refractive index detector (40 °C). Injection volume used was 50 μL. The column set used was a set of three PLgel mixed-C columns (5 μm particles, 300 × 7.5 mm each) (40 °C) in series with a flow rate of 1.0 mL/min. Data acquisition and processing software were Waters Empower2 (all detectors) and Viscotek Omnisec4 (LS, Visco and Waters DRI detection). All samples were filtered (0.2 μm PTFE filter, 17 mm, PP housing, Alltech) prior to the measurements.

Transmission electron microscopy (TEM) was performed on a FEI Technai 20 (type sphera) with a operating voltage 200 kV, LaB6 filament and a bottom mounted Gatan CCD camera (1K × 1K). The samples were prepared from a 2 mg/mL dichloromethane/DMF (50/50) solution casted on carbon-coated 200-mesh grids (freshly glow discharged) and dried overnight.

Dynamic light scattering (DLS) was performed on a Malvern zetasizer nano zs, equipped with a 4 W, 633 nm He−Ne. Detection was performed at a 90° angle to the incident beam. The peptide-conjugated nanoparticles were dissolved in DMF 24 h prior to the measurements. The hydrodynamic radii (*z*-average, monomodal distribution) were determined at 20 °C as a function of the concentration varying from 0.15 to 8.0 mg/mL. The calculations were performed with the Malvern software.

Cryogenic transmission electron microscopy (cryo-TEM) measurements were performed on a FEI Tecnai 20, type Sphera TEM instrument (with a LaB6 filament, operating voltage = 200 kV). The sample vitrification procedure was performed using an automated vitrification robot (FEI Vitrobot Mark III). A 3 μL sample was applied to a Quantifoil grid (R 2/2, Quantifoil Micro Tools GmbH; freshly glow discharged for 40 s just prior to use) within the environmental chamber of the Vitrobot, and the excess liquid was blotted away. The thin film thus formed was shot into melting ethane. The grid containing vitrified film was immediately transferred to a cryoholder (Gatan 626) and observed under low dose conditions at −170 °C.

Synthesis of NCA of γ-Benzyl-L-glutamate[33]. Both α-pinene (5.74 g, 42.14 mmol) and γ-benzyl-L-glutamate (5.00 g, 21.07 mmol) were dissolved and suspended, respectively, in distilled ethyl acetate (40 mL) in a three-neck round-bottom flask. The mixture was stirred and heated under reflux at 76 °C. To this a triphosgene solution (3.13 g, 10.54 mmol) in ethyl acetate (20 mL) was added dropwise. Two-thirds of the solution was added in 1 h, the reaction was left for another hour, and then some additional triphosgene solution was added until everything dissolved. The reaction mixture was concentrated to 2/3 in vacuo, and the same amount of *n*-heptane was added. The mixture was allowed to cool to room temperature and was further cooled in the freezer. After filtration, the solid was washed three times with a 1:4 ethyl acetate/*n*-heptane solution. After filtration the solid was further purified by freeze-drying and stored in a freezer (−18 °C) over P_2O_5 until used. Yield: 4.20 g (83%); mp = 94 °C. ^{1}H NMR (400 MHz, $CDCl_3$): 9.07 ppm (s, 1H), 7.34 (m, 5H), 4.45 ppm (q, 1H), 2.50 ppm (t, 2H), 1.96 ppm (m, 2H).

PBLG Macroinitiator. The bifunctional nitroxide initiator and γ-benzyl-L-glutamate NCA were weighed in a 250 mL three-neck flask at molar ratios of 1:20 and 1:40. The flask was placed in a refrigerated saltwater tank of −2.0 °C. To the mixture 75 mL of cold (4 °C) dry DMF was added, and the reaction was maintained for 4 or 5 days under an inert atmosphere. The solution was precipitated in isopropyl alcohol and placed in the refrigerator overnight at 4 °C. By filtration a white solid polymer was collected. The isolated yields were around 75%.

PBLG−PS Block Copolymers. The macroinitiator (initiator-PBLG) was weighed in a Schlenk tube, and dry DMF was added. Distilled styrene was added for the desired PBLG to styrene ratio (20:1 or 40:1, respectively). Oxygen was removed with three freeze−thaw cycles, and the reaction was maintained at 125 °C for 16 h under argon. After cooling the sample, the polymer was precipitated in methanol. After filtration a white powder was obtained. Yield: 80%.

Cross-Linking of Block Copolymer with Styrene and Divinylbenzene. The PBLG−PS block copolymer (1 g) was weighed into a Schlenk tube, and dry DMF was added (10 mL). Distilled divinylbenzene (technical grade, 80%) was added in the desired cross-linker to initiator ratio (10:1 to 50:1), and oxygen was removed with three freeze−thaw cycles. The reaction was maintained at 125 °C for 18 h under argon. After cooling the sample, the polymer was precipitated in methanol, and after filtration a white powder was obtained. Yield: 1 g.

Deprotection of the Core−Shell Particles. The polymer (0.5 g) was dissolved in DMF (20 mL), and 0.05 g of Pd/C was added. The mixture was placed in a Parr reactor, and 5 Atm of H_2 was applied. In the first 6 h, the pressure was adjusted to 5 Atm, and after that, the reaction was maintained for another 18 h. The reaction mixture was taken out of the reactor, the mixture was filtered through a 0.2 μm filter, and the filtrate was concentrated to 7 mL under vacuum. The concentrated solution of deprotected polymer particles was precipitated in petroleum ether (50 mL). The polymers were collected by filtration and were dried prior to analysis.

Results and Discussion

The synthetic reaction sequence toward the peptide-conjugated nanoparticles is depicted in Scheme 1. Well-defined polypeptide macroinitiators can be synthesized by the polymerization

Scheme 1. Synthetic Approach to Functional Cross-Linked Polypeptide Core−Shell Nanopaticles: (1) Synthesis of PBLG Macroinitiator with Nitroxide End-Groups; (2) Synthesis of PBLG−PS Block Copolymer with Nitroxide End-Groups; (3) Cross-Linking of Block Copolymers in the Presence of DVB; (4) Deprotection of PBLG Shell

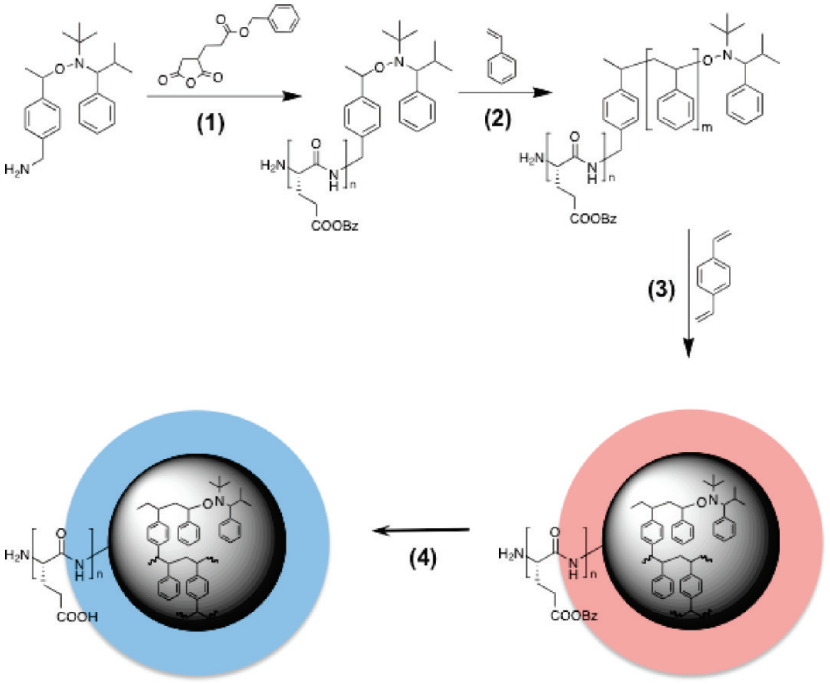

of γ-benzyl-L-glutamate (BLG) *N*-carboxyanhydride (NCA) from a heterofunctional initiator.[34,35] The initiator employed here contains a primary amine acting as an initiating moiety for NCA polymerization and a nitroxide group for controlled radical polymerization.[36] In the second step, initiation of styrene from the PBLG macroinitiator yielded a well-defined rod−coil block copolymer. The final formation of the peptide-conjugated nanoparticles was facilitated by the reaction of the active chain end of the block copolymer with a cross-linker (divinylbenzene). Using this arm-first approach is promising because the reaction is performed in individual steps. This makes it possible to control each step, for example, the block length ratio of the α-helical polypeptide segment and the polystyrene block by varying the monomer to (macro)initiator molar ratio ([M]/[I]). We hypothesized that the block length ratio as well as the amount of cross-linker used in the final step of the reaction would have an influence on the product morphology. To develop an optimized synthetic protocol and to verify the hypothesis, a systematic synthetic approach was followed. First, PBLG of two different degrees of polymerization was synthesized, i.e., 20 and 40, respectively. Each PBLG macroinitiator was extended with 20 or 40 monomer units of styrene to obtain four different block copolymers, i.e., PBLG(20)−PS(20), PBLG(20)−PS(40), PBLG(40)−PS(20), and PBLG(40)−PS(40). Finally, each macroinitiator was cross-linked with five different block copolymer to cross-linking agent molar ratios varying from 1:10 to 1:50.

Block Copolymer Synthesis. The detailed synthesis of P(BLG-*b*-S) using the heterofunctional initiator was described in a previous publication.[36] Therefore, the following discussion will only briefly summarize the results. The NCA polymerization was performed at 0 °C in DMF, which allows good control over the polymer end-group, molecular weight, and polydispersity index (PDI).[35,37−40] Accordingly, PBLGs with low PDI (1.1) were obtained in high yields without any loss of the nitroxide end-group as was evident from MALDI-ToF analysis. Size exclusion chromatography (SEC) revealed monomodal traces with number-average molecular weights of 4100 g/mol for the PBLG(20) and 8100 g/mol for the PBLG(40). Subsequent macroinitiation from both PBLGs using two different ratios of PBLG to styrene yielded four block copolymers displaying the expected increase in molecular weight and low PDIs of 1.1 (Table 1). Because of the different contribution of the rod and coil segments to the hydrodynamic volume, the absolute molecular weights were determined using universal calibration (Table 1). From the results it can be seen that the styrene macroinitiation from the PBLG(20) (M_n = 4100 g/mol) leads to a molecular weight of 6500 and 8600 g/mol for the PBLG(20)−PS(20) and PBLG(20)−PS(40), respectively. A similar agreement with the expected increase in molecular weight was observed for the PBLG(40) polymers (Table 1). Figure 1 shows the example of the SEC traces of the PBLG(20) and the resulting block copolymers. A clear shift to higher molecular weight is observed after initiation for the two different PBLG to styrene ratios. As already discussed in our previous paper, all SEC traces of the block copolymers show a small second peak at high molecular weight, which is the result of radical−radical coupling of two growing polymer chains (Figure 1).[36] However, this is not expected to cause any problem in the cross-linking step, as these chains cannot participate in this reaction due to the lack of an active chain-end and are consequently removed in the product purification step.

Table 1. Molecular Weights and Polydispersity Indices (PDI) of the PBLG Macroinitiators and Block Copolymers[a]

entry	polymer	M_n (g mol^{-1})	P_n (PBLG/PS)	M_w (g mol^{-1})	PDI
1	PBLG(20)	4100	20/0	4400	1.1
2	PBLG(20)−PS(20)	6500	20/23	7300	1.1
3	PBLG(20)−PS(40)	8600	20/43	9500	1.1
4	PBLG (40)	8100	40/0	9700	1.1
5	PBLG(40)−PS(20)	9900	40/16	11000	1.1
6	PBLG(40)−PS(40)	12200	40/39	13400	1.1

[a] Numbers in parentheses refer to the targeted degree of polymerization. All data were determined by SEC in DMF with universal calibration.

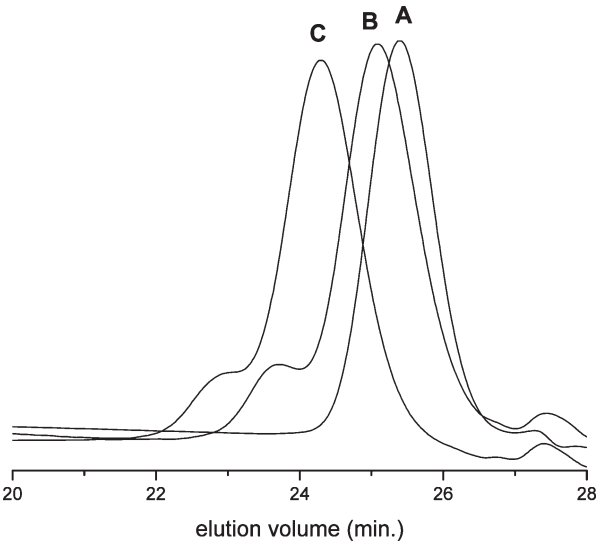

Figure 1. SEC traces of PBLG macroinitiator (A; entry 1, Table 1), PBLG(20)−PS(20) (B; entry 2, Table 1), and PBLG(20)−PS(40) (C; entry 3, Table 1).

Formation of Peptide-Conjugated Nanoparticle. As shown by Matyjaszewski for ATRP, by varying the concentration of active polymer chains to cross-linker like divinylbenzene (DVB), the size and morphology of the resulting star polymers can be influenced.[30] To investigate the applicability of this approach for peptide block copolymers, we systematically varied the ratio of DVB to block copolymer for all block copolymers listed in Table 1. The use of pure p-DVB was not desired in this reaction since its purification is a tedious procedure, and due to its high reactivity, the storage and handling of pure DVB can be problematic. Instead, commercial, technical grade DVB was used, which contains approximately 55% *m*-DVB and 25% *p*-DVB, less than 17% of *m*- and *p*- ethylvinylbenzene, and less than 1% *o*-, *m*-, and *p*-diethylbenzene. This means that only around 80% of the technical grade DVB is available for cross-linking, 17% can polymerize but not cross-link, and 1% is not able to polymerize at all. In control experiments we confirmed that technical grade DVB can be used directly for this process without further purification.

Initially, the cross-linking reaction was attempted with block copolymers containing 20 PBLG residues and DVB to block copolymer molar ratios ranging from 10:1 to 50:1, taking into account that technical grade DVB contains only 80% difunctional monomers. All polymerizations were carried out with 1 g of block copolymer and the calculated amount of DVB in 5 mL of DMF for 18 h at 125 °C. The cross-linking of both block copolymers, i.e., PBLG(20)−PS(20) and PBLG(20)−PS(40), was successful for block copolymer to DVB ratios up to 20:1 (Table 2). As expected, the molecular weight of the polymers obtained with higher cross-linker to block copolymer ratios are higher than for lower ratios. For example, in the case of PBLG(20)−PS(40), number-average molecular weights of 135 000 and 384 000 g/mol were found for the DVB-to-macroinitiator molar ratios of 10:1 and 20:1, respectively. The higher PDI of the latter (1.8) clearly indicates that by increasing the ratio cross-linker to block copolymer the control over the polymerization is reduced. For higher ratios, gelation occurred, and further analysis of the polymers was not possible. This is in agreement with studies of Hawker, who found a general molecular weight dependency for NMP cross-linking reactions by high throughput experimentation.[41] For macroinitiators with low molecular weights, a low molar ratio of DVB to macroinitiator was sufficient to obtain well-defined star polymers, since low molecular weight macroinitiators are more prone to cross-linking. In our case also other factors could play a role during cross-linking, for example, inter- and intramolecular hydrogen bonding of peptide blocks. For instance, PBLG blocks shorter than 18 monomer residues are not completely in the α-helix conformation but can resemble β-sheet structures.[42] This can result in intermolecular interactions, which give rise to agglomeration and could finally contribute to the gel formation. Even the use of a hydrogen bond breaking solvent like DMF does probably not completely prevent such interaction.[43]

Table 2. Number-Average (M_n) and Weight-Average (M_w) Molecular Weights of the Polymers Obtained after Cross-Linking of the PBLG−PS Block Copolymers with Various Block Length and Block Copolymer to DVB Molar Ratio[a]

entry	block copolymer	ratio DVB:MI	M_n (10^3 g mol^{-1})	M_w (10^3 g mol^{-1})	PDI
1	PBLG(20)−PS(20)	9.8	115 000	156 000	1.4
2	PBLG(20)−PS(40)	17.7	315 000	589 000	1.9
3	PBLG(20)−PS(20)	11.8	135 000	182 000	1.3
4	PBLG(20)−PS(40)	17.0	384 000	687 000	1.8
5	PBLG(40)−PS(20)	11.2	54 000	77 000	1.4
6	PBLG(40)−PS(20)	19.5	123 000	166 000	1.4
7	PBLG(40)−PS(20)	30.5	238 000	320 000	1.4
8	PBLG(40)−PS(20)	43.0	277 000	380 000	1.4
9	PBLG(40)−PS(20)	51.0	281 000	399 000	1.4
10	PBLG(40)−PS(40)	10.4	47 000	79 400	1.7
11	PBLG(40)−PS(40)	23.3	122 000	181 000	1.5
12	PBLG(40)−PS(40)	33.3	278 000	383 000	1.4
13	PBLG(40)−PS(40)	41.9	428 000	595 000	1.4
14	PBLG(40)−PS(40)	50.8	548 000	819 000	1.5

[a] The values were determined after fractional precipitation.

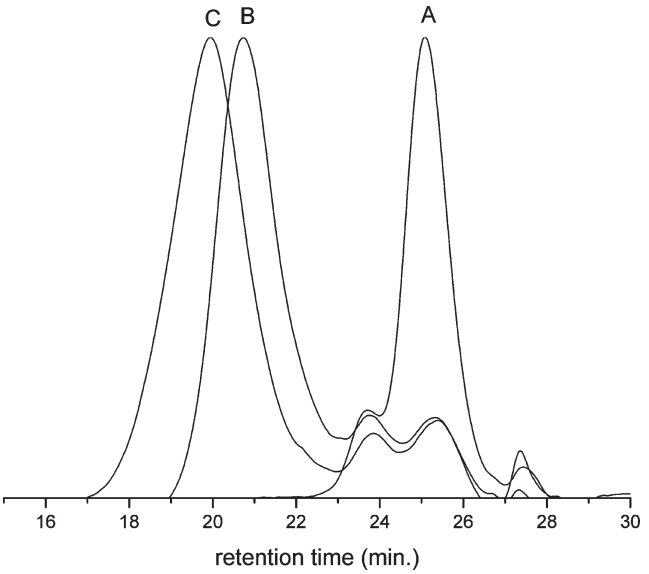

Figure 2. DMF-SEC traces of cross-linked polymers obtained from PBLG(20)−PS(20) (A) at DVB to block copolymer molar ratio 10:1 (B) and 20:1 (C).

Analysis of the SEC chromatograms of the soluble materials revealed that after 18 h of reaction still some block copolymer remained in both systems as well as the shoulder corresponding to the higher molecular weight peak of the block copolymer (Figure 2). An obvious explanation for the remaining unreacted block copolymer would be that the reaction time was simply not sufficient. However, from the SEC traces it can also be seen that with increasing molar ratio DVB to block copolymer the amount of unreacted starting

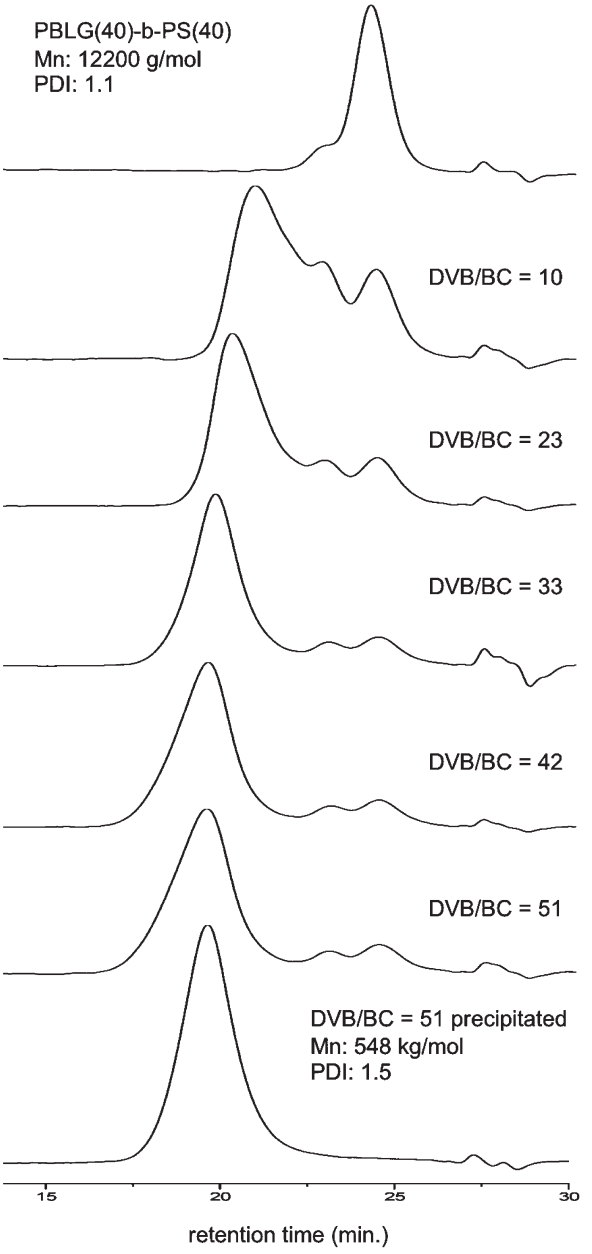

Figure 3. DMF-SEC traces of polymers obtained from cross-linking of PBLG(40)−PS(40) with different DVB to block copolymer (BC) molar ratios.

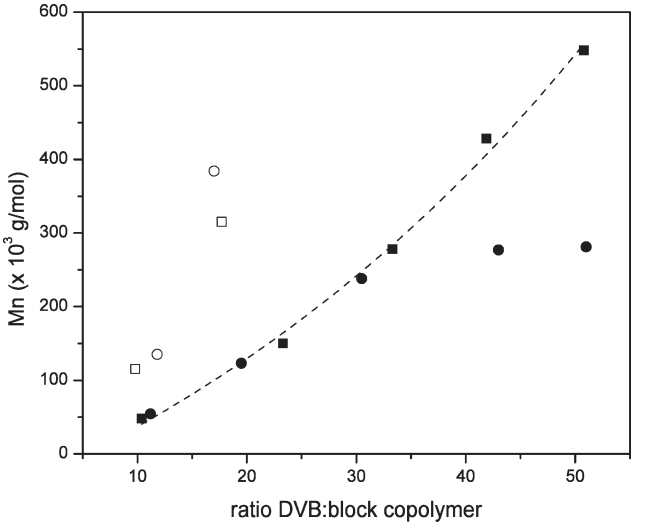

Figure 4. Molecular weight as a function of DVB to block copolymer molar ratio for PBLG(20)−PS(20) (○), PBLG(20)−PS(40) (□), PBLG(40)−PS(20)) (●), and PBLG(40)−PS(40)) (■, dotted line added to guide the eye).

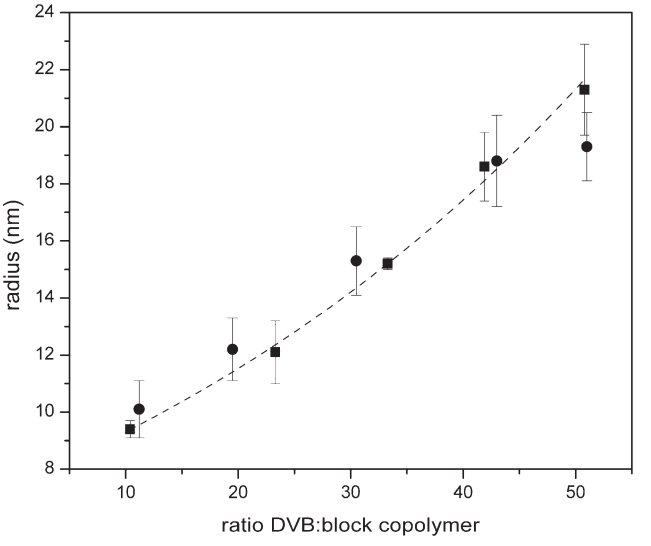

Figure 5. Hydrodynamic radius determined by dynamic light scattering as a function of DVB to macroinitiator molar ratio for the P(BLG(40)-*b*-S(20)) system (●) and for the P(BLG(40)-*b*-S(40)) system (■, dotted line added to guide the eye).

materials remains constant. This indicates that the amount and size of the formed nanoparticles were not sufficient to accommodate all block copolymers. Hawker also found up to 1−2% of their macroinitiator remaining in the final star polymer.[41] Matyaszewski found for a comparable system, initiated by ATRP, an incorporation of 95% of all the chains, thus 5% remaining starting material.[30] By the addition of extra monofunctional monomers, thereby increasing the core size, they were able to incorporate an additional amount of macroinitiator. Although both mentioned studies were done with coil-like macroinitiators and not with rod−coil systems, they suggest that it is a question of spacial constraints rather than of reaction time. Increasing the core size should therefore result in more complete incorporation of block copolymers.

Significantly better results were indeed obtained for the block copolymers consisting of 40 γ-benzyl-L-glutamate residues. In contrast to the results obtained from the block copolymers containing 20 monomer units in the PBLG block, gelation was never observed, not even at DVB to block copolymer molar ratios of 50:1. Figure 3 shows the SEC traces of the PBLG(40)−PS(40) cross-linking reaction after 18 h with different DVB ratios. A pronounced shift of the traces to higher molecular weight with an increasing DVB to block copolymer ratio as compared to the initial block copolymer is evident. While all samples show unreacted block copolymer, the amount appears relatively small and constant at a DVB/BC molar ratio >23. This unreacted starting material can be removed by fractional precipitation. Considering the applied chemistry, the relatively low polydispersity of the cross-linked polymers around 1.5 and the symmetric shape of the SEC traces at higher DVB/BC ratios is remarkable. This suggests a reasonably controlled cross-linking process. Table 1 (entries 5−14) summarizes the molecular weights and DPIs obtained for

PBLG(40)-based reactions. Interesting is the comparison of the molecular weights obtained in all reactions as a function of the block length and the DVB/BC ratio. Inspection of Figure 4 reveals several trends. For the largest block copolymer (PBLG(40)−PS(40)) the molecular weight increases almost linearly up to 548 000 g/mol with increasing DVB/BC molar ratio while the PBLG(40)−PS(20) system reaches a plateau molecular weight for DVB/PS molar ratios >30 at about 280 000 g/mol. This is believed to be due to the higher molecular weight of the styrene block of the macroinitiator, which results in a larger cross-linked PS core. A larger core can accommodate more block copolymers, but it can be expected that the PBLG(40)−PS(40) will reach a plateau as well, yet at higher DVB concentrations.

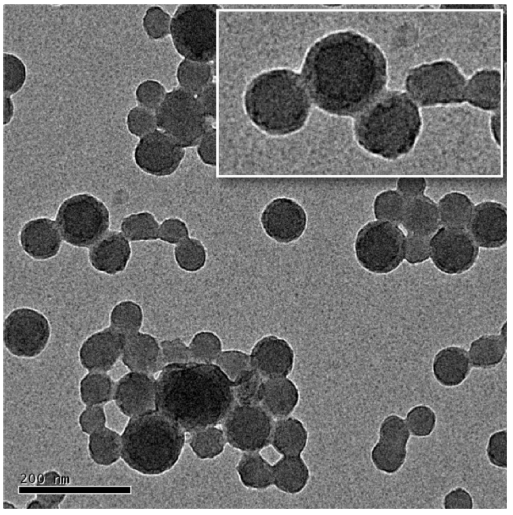

Figure 6. Transmission electron microscope picture of peptide core/shell nanoparticle obtained from PBLG(40)−PS(40) with a DVB to macroinitiator molar ratio of 50:1 (Table 2, entry 14).

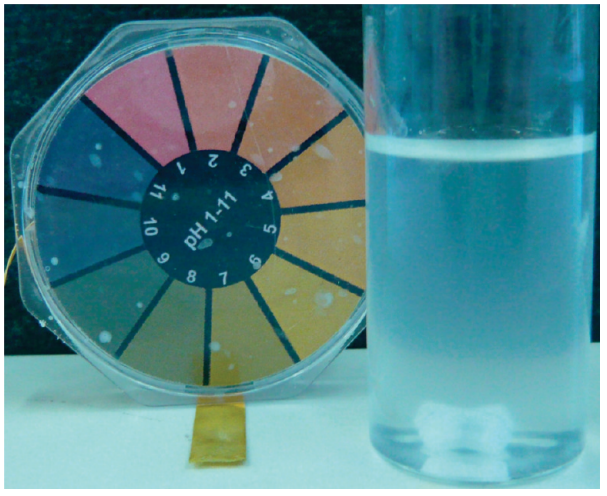

Figure 7. Suspension of deprotected peptide core cross-linked nanoparticles from PBLG(40)−PS(40) in water at pH = 8.

Moreover, when the results of the PBLG(40) block copolymer are compared to the results obtained from the systems consisting of 20 γ-benzyl-L-glutamate units, it can be seen that the obtained molecular weight of the latter are much higher for the same DVB:BC molar ratio.

The hydrodynamic radii of all cross-linked polymers were determined by dynamic light scattering as a function of concentration at 20 °C. The consistency of the measured radii at all investigated concentrations implies that the cross-linked core−shell particles were below their critical overlap concentration, and thus the radii could be determined with good accuracy. Figure 5 depicts the averaged radii of the particles obtained from the PBLG(40) series. The trend of increasing particle size with increasing DVB/BC ratio is consistent with the SEC results (Figure 4). The particles sizes increase from 9 to 21 nm for the PBLG(40)−PS(40) system with increasing DVB to block copolymer molar ratio. While not as apparent as in the SEC plot, the PBLG(40)−PS(20) system levels off to a plateau, yet at an apparently higher DVB/BC ratio. The light scattering results also suggest a larger particle polydispersity than the SEC results.

The core−shell structure of the nanoparticles was visualized by transmission electron microscopy (TEM). The micrograph in Figure 6 shows the example of particles formed from the PBLG(40)−PS(40)) with the highest DVB to macroinitiator molar ratio (50:1). The particles present a clear contrast between the dark core surrounded by a gray shell. It is reasonable to assume that the core is PS and the periphery is composed of PBLG. It can, however, not be excluded that some PBLG is captured in the core of the particle. It also becomes clear that the particle sizes, which were determined by light scattering, are in good agreement with the size of the particles as visualized in the TEM micrographs and that the particles vary in size.

Responsive Particles. In order to obtain responsive core−shell nanoparticles, the benzyl protecting group of the PBLG must be removed. This was expected to produce a pH-responsive poly(L-glutamic acid) shell around the PS core. The deprotection was carried out on the PBLB(40)−PS(40) (Table 2, entry 14) and on the particle PBLB(40)−PS(20) (Table 2, entry 9) with Pd/C and H_2 for 24 h. Although it was not possible to monitor the deprotection spectroscopically

Scheme 2. Depiction of pH Responsive Peptide-Based Core−Shell Nanoparticles Assuming a Helix−Coil Transition by pH Change

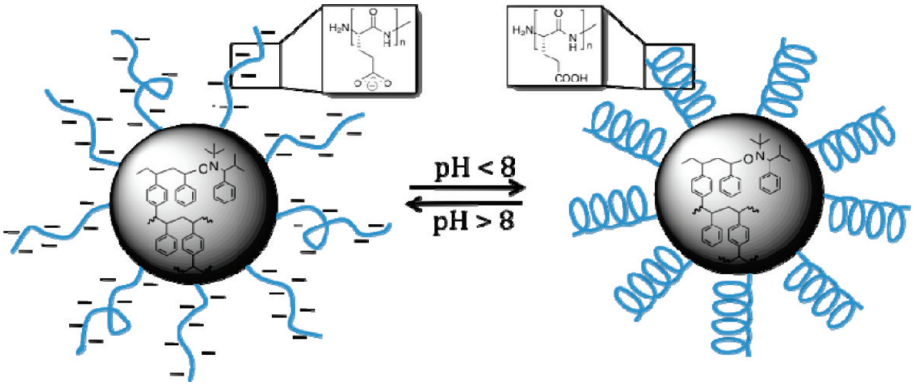

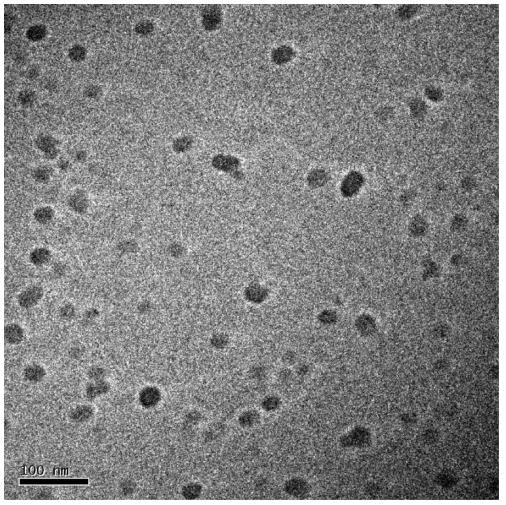

Figure 8. Cryo-TEM of deprotected core−shell nanoparticles in water pH = 11.

and the extent of the deprotection could thus not be quantified, the hydrophilicity and solubility of the nanoparticles clearly changed. The previously hydrophobic materials were now readily water dispersible at pH > 8, at which deprotonation of the poly(L-glutamic acid) (PGA) takes place (Figure 7). When the pH was lowered, the reprotonation of the PGA resulted in a (reversible) precipitation of the nanoparticles from the aqueous solution. While a conformational change from helix to coil was not monitored directly on the particles, Iizuka reported that poly(L-glutamic acid) goes through a helix−coil transition by changing the pH and behaves like a random coil electrolyte at higher pHs (Scheme 2).[44] Cryo-TEM pictures taken of the aqueous solution at pH = 11 confirm that the particles are individually dispersed (Figure 8). Moreover, a white corona can be seen around the particles, which is believed to be the solvated polyelectrolyte-like poly(L-glutamic acid) shell.

Conclusions

We have shown that well-defined bioconjugated polymeric nanoparticles with a core−shell structure can be obtained from polypeptide (PBLG) block copolymers with active controlled radical initiator end-groups. The latter allow the cross-linking of the block copolymers in the presence of difunctional monomers. A clear effect of the block length ratio and amount of cross-linker in the process was observed. While gel formation occurred even at low block copolymer to cross-linker molar ratio for shorter block copolymers, individual core shell particles were synthesized from longer block copolymers for the whole range of tested ratios. Particles with a molecular weight up to 595 000 g/mol (SEC) and 21 nm (DLS) size were obtained. Deprotection of the PBLG yielded pH responsive particles with a poly(L-glutamic acid) shell and a polystyrene core. We believe that this method is generally applicable to the synthesis of bioconjugated core−shell particles.

Acknowledgment. Funding for this work was provided by the "Netherlands Organisation for Scientific Research" (NWO) and the "Deutsche Forschungsgemeinschaft" (DFG). The authors also thank Rinske Knoop for cryo-TEM measurements. A.H. thanks the Science Foundation Irland for support under Grant 07/SK/B1241.

References and Notes

(1) Klok, H.-A. *J. Polym. Sci., Part A: Polym. Chem.* **2005**, *43*, 1.
(2) Osada, K.; Kataoka, K. *Adv. Polym. Sci.* **2006**, *202*, 113.
(3) Rothenfluh, D. A.; Bermudez, H.; O'Neil, C.; Hubbell, J. A. *Nat. Mater.* **2008**, *7*, 248.
(4) Lutolf, M. P.; Weber, F. E.; Schmoekel, H. G.; Schense, J. C.; Kohler, T.; Müller, R.; Hubbell, J. A. *Nat. Biotechnol.* **2003**, *21*, 513.
(5) Rathore, O.; Sogah, D. Y. *J. Am. Chem. Soc.* **2001**, *123*, 5231.
(6) Hentschel, J.; Börner, H. G. *Macromol. Biosci.* **2009**, *9*, 187.
(7) Kaparov, P.; Antonietti, M.; Cölfen, H. *Colloids Surf., A* **2004**, *250*, 153.
(8) Guo, X.-H.; Yu, S.-H.; Cai, G.-B. *Angew. Chem., Int. Ed.* **2006**, *45*, 3977.
(9) Klok, H.-A. *Macromolecules* **2009**, *42*, 7990.
(10) Daniel, M. C.; Astruc, D. *Chem. Rev.* **2004**, *104*, 293.
(11) Elghanian, R.; Storhoff, J. J.; Mucic, R. C.; Letsinger, R. L.; Mirkin, C. A. *Science* **1997**, *277*, 1078.
(12) Santra, S.; Yang, H.; Dutta, D.; Stanley, J. T.; Holloway, P. H.; Tan, W.; Moudgil, B. M.; Mericle, R. A. *Chem. Commun.* **2004**, 2810.
(13) Wu, P.; He, X.; Wang, K.; Tan, W.; Ma, D.; Yang, W.; He, C. J. *Nanosci. Nanotechnol.* **2008**, *8*, 2483.
(14) Aili, D.; Enander, K.; Rydberg, J.; Nesterenko, I.; Bjoerefors, F.; Baltzer, L.; Liedberg, B. *J. Am. Chem. Soc.* **2008**, *130*, 5780.
(15) Kricheldorf, H. R. *Angew. Chem., Int. Ed.* **2006**, *45*, 572.
(16) Hadjichristidis, N.; Iatrou, H.; Pitskalis, M.; Sakellariou, G. *Chem. Rev.* **2009**, *109*, 5528.
(17) Deming, T. J. *Adv. Polym. Sci.* **2006**, *202*, 1.
(18) Schlaad, H. *Adv. Polym. Sci.* **2006**, *202*, 53.
(19) Klok, H.-A.; Lecommandoux, S. *Adv. Polym. Sci.* **2006**, *202*, 75.
(20) Karatzas, A.; Iatrou, H.; Hadjichristidis, N.; Inoue, K.; Sugiyama, K.; Hirao, A. *Biomacromolecules* **2008**, *9*, 2072.
(21) Babin, J.; Rodriguez-Hernandez, J.; Lecommandoux, S.; Klok, H.-A.; Achard, M.-F. *Faraday Discuss.* **2005**, *128*, 179.
(22) Checot, F.; Lecommandoux, S.; Klok, H. A.; Gnanou, Y. *Eur. Phys. J. E* **2003**, *10*, 25.
(23) Gebhardt, K. E.; Ahn, S.; Venkatachalam, G.; Savin, D. A. *Langmuir* **2007**, *23*, 2851.
(24) Dibbern, E. M.; Toublan, F. J.-J.; Suslick, K. S. *J. Am. Chem. Soc.* **2006**, *128*, 6540.
(25) Uchino, H.; Matsumura, Y.; Negishi, T.; Koizumi, F.; Hayashi, T.; Honda, T.; Nishiyama, N.; Kataoka, K.; Naito, S.; Kakizoe, T. *Br. J. Cancer* **2005**, *91*, 678.
(26) O'Reilly, R. K.; Hawker, C. J.; Wooley, K. L. *Chem. Soc. Rev.* **2006**, *35*, 1068.
(27) Rosler, A.; Vandermeulen, G. W.; Klok, H. A. *Adv. Drug Delivery Rev.* **2001**, *53*, 95.
(28) Bousquet, A.; Perrier-Cornet, R.; Ibarboure, E.; Papon, E.; Labrugere, C.; Heroguez, V.; Rodriguez-Hernandez, J. *Biomacromolecules* **2008**, *9*, 1811.
(29) Bosman, A. W.; Vestberg, R.; Heumann, A.; Fréchet, J. M.; Hawker, C. J. *J. Am. Chem. Soc.* **2003**, *125*, 715.
(30) Gao, H.; Matyjaszewski, K. *Macromolecules* **2006**, *39*, 3154.
(31) Barner-Kowollik, C.; Davis, T. P.; Stenzel, M. H. *Aust. J. Chem.* **2006**, *59*, 719.
(32) Benoit, D.; Chaplinski, V.; Braslau, R.; Hawker, C. J. *J. Am. Chem. Soc.* **1999**, *121*, 3904.
(33) Cornille, F.; Copier, J.-L.; Senet, J.-P.; Robin, Y. EP 1 201 659 A1.
(34) Steig, S.; Cornelius, F.; Witte, P.; Koning, C. E.; Heise, A.; Menzel, H. *Chem. Commun.* **2005**, *43*, 5420.
(35) Habraken, G. J. M.; Koning, C. E.; Heise, A. *J. Polym. Sci., Part A: Polym. Chem.* **2009**, *47*, 6883.
(36) Knoop, R. J. I.; Habraken, G. J. M.; Gogibus, N.; Steig, S.; Menzel, H.; Koning, C. E.; Heise, A. *J. Polym. Sci., Part A: Polym. Chem.* **2008**, *46*, 3068.
(37) Vayaboury, W.; Giani, O.; Cottet, H.; Deratani, A.; Schué, F. *Macromol. Rapid Commun.* **2004**, *25*, 1221.
(38) Habraken, G. J. M.; Heuts, J. P. A.; Koning, C. E.; Heise, A. *Chem. Commun.* **2009**, 3612.
(39) Vayaboury, W.; Giani, O.; Cottet, H.; Bonaric, S.; Schué, F. *Macromol. Chem. Phys.* **2008**, *209*, 1628.
(40) Habraken, G. J. M., Peeters, M.; Dietz, C. H. J. T.; Koning, C. E.; Heise, A. *Polym. Chem.* **2010**, DOI 10.1039/b9py00337a.
(41) Bosman, A. W.; Heumann, A.; Klaerner, G.; Benoit, D.; Frechet, J. M. J.; Hawker, C. J. *J. Am. Chem. Soc.* **2001**, *123*, 6461.
(42) Papadopoulos, P.; Floudas, G.; Klok, H. A.; Schnell, I.; Pakula, T. *Biomacromolecules* **2004**, *5*, 81.
(43) Doty, P.; Bradbury, J. H.; Holtzer, A. M. *J. Am. Chem. Soc.* **1956**, *78*, 947.
(44) Iizuka, E.; Yang, J. T. *Biochemistry* **1965**, *4*, 1249.